

Suppressed Carrier Synchronizers for ISI Channels¹

Sami M. Hinedi, Marvin K. Simon

Jet Propulsion Laboratory, California Institute of Technology
4800 Oak Grove Drive, Pasadena, CA 91109 USA
email: marvin.k.simon@jpl.nasa.gov

Abstract

We demonstrate a class of suppressed carrier synchronization loops that are motivated by MAP estimation theory and in the presence of ISI outperform the conventional I-Q loop which is designed on the basis of zero ISI (wideband assumption.) The measure of comparison used is the so-called "squaring loss" (the reduction in loop SNR relative to that of a phase-locked loop (PLL) of the same loop bandwidth). Equivalently, comparisons will be made on the basis of mean-squared phase jitter for equal loop bandwidths and signal power to noise power spectral density ratios. Although the specific results presented in this paper are derived for binary phase-shift-keying (BPSK), the paper begins by considering a more general I-Q form of modulation which allows for such techniques as quaternary phase-shift-keying (QPSK) and quadrature amplitude modulation (QAM). Detailed extensions to these more general modulation forms are straightforward and readily obtained in view of results previously presented in the literature.

¹The authors are with the Jet Propulsion Laboratory, Pasadena, CA. The work was performed both at the University of Southern California and under a contract to the National Aeronautics and Space Administration.

Suppressed Carrier Synchronizers for ISI Channels¹

Sami M.J. Inedi, Marvin K. Simon

Jet Propulsion Laboratory, California Institute of Technology
4800 Oak Grove Drive, Pasadena, CA 91109 USA
email: marvin.k.simon@jpl.nasa.gov

1. Introduction

The problem of suppressed carrier synchronization (sync) in digital coherent communication systems has received widespread attention over the years both from a theoretical as well as a practical point of view. In reality, these two points of view are not separate from each other in that the carrier sync structures that are commonly employed in the design of coherent receivers are those that are motivated by the application of the maximum a posteriori (MAP) estimation theory. Although evidence of such a relation can be found in many of the literature citations, a recent expose of the subject [1] clearly points out this association between the teachings of the theory and what is commonly accepted as today's practice while at the same time providing further insight. Indeed, it was pointed out in [1] that the purpose of documenting the results was not to reinvent the wheel but rather to add some new spokes to it.

Common to [1] and the myriad of papers on the subject that preceded it is the fact that carrier synchronization was viewed as a problem to be solved independent of any bandwidth limitations imposed on the system. In particular, the carrier sync structures (open and closed loop) that have been derived and classified as being "optimum" in the sense of being motivated by MAP estimation theory are

¹The authors are with the Jet Propulsion Laboratory, Pasadena, CA. The work was performed both at the University of Southern California and under a contract to the National Aeronautics and Space Administration.

wideband structures and ignore the presence of intersymbol interference (ISI), the latter being handled independently in the receiver by the inclusion of some form of equalization. In fact, much of the work on suppressed carrier closed loop synchronization that has appeared in the technical journals and textbooks and is described in terms of the well known Costas loop or Inphase Quadrature (I-Q) loop [2,3] assumes a rectangular signaling pulse of duration equal to one symbol interval which appears undistorted at the input of the receiver.

In this paper, we revisit the carrier sync problem with emphasis on finding "optimum" (in the sense of being motivated by MAP estimation theory) closed loop structures when ISI is present at the receiver input. To the authors' knowledge, very little has been reported on this subject other than the treatment presented in [4] (which was heretofore not published). Prior to that, the only other work that the authors are aware of that dealt with ISI effects on suppressed carrier synchronization appeared in [5,6]. The primary purpose of this paper is to reexamine the work performed in [4] in the light of removing certain restrictions that were placed on the problem thereby allowing improved justification for some of the assumptions made therein as well for the results obtained based on these assumptions. In particular, we shall derive and analyze the performance of a class (depending on the time duration of the observable) of carrier sync structures that outperform the conventional (zero ISI) I-Q Costas loop when ISI is present in the receiver input signal. Emphasis will be placed on ease of implementation and low cost of these loops. The amount by which these "ISI-compensated I-Q loops" outperform the conventional I-Q loop will be assessed by comparing the so-called "squaring loss" (the reduction in loop SNR relative to that of a phase-locked loop (PLL) of the same loop bandwidth) of the various configurations of the former with that of the latter. Equivalently, comparisons will be made on the basis of mean-squared phase jitter for equal loop bandwidths and signal power to noise power spectral density ratios.

Although the specific results presented in this paper are derived for binary phase-shift-keying (BPSK), we shall begin by considering a more general I-Q form of modulation which allows for such techniques as quaternary phase-shift-keying (QPSK) and quadrature amplitude modulation (QAM). Detailed extensions to these more general modulation forms are straightforward and readily obtained in view of the previous results presented in [4].

2. System and Signal Model

The general digital communication transmitter model considered here is illustrated in Fig. 1. In this figure, $g(t)$ is assumed to be a unit power rectangular pulse of duration T sec (a single baud) and $h(t)$ is the impulse response of a pulse-shaping filter that spreads $g(t)$ beyond a single baud interval and accounts for the ISI seen at the input to the receiver. Letting $p(t) = g(t) * h(t)$ denote the spread pulse, then the I-Q carrier modulated signal seen at the input to the receiver can be written in the form

$$s(t, \theta) = A [m_I(t) \cos(\omega_c t + \theta) - m_Q(t) \sin(\omega_c t + \theta)] \quad (1)$$

where A is the signal amplitude and

$$m_I(t) = \sum_{k=-\infty}^{\infty} a_k p(t - kT); \quad m_Q(t) = \sum_{k=-\infty}^{\infty} b_k p(t - kT) \quad (2)$$

with $\{a_k\}$ and $\{b_k\}$ respectively denoting the streams of independent I and Q data symbols. For the case of BPSK, either $m_I(t)$ or $m_Q(t)$ equals zero and the data symbols of the remaining modulation take on values ± 1 . In this case, $A^2/2 = P$ denotes the signal power in watts. In addition to the signal in (1) the additive noise $n(t)$ present at the receiver input is characterized as a bandlimited white Gaussian noise process with single-sided power spectral density N_0 watts/Hz.

3. The MAP Estimation of Carrier Phase

Based on an observation of the received signal plus noise $r(t) = s(t, \theta) + n(t)$ over a time interval \mathcal{Y} , we wish to estimate the random parameter θ (assumed to be time

invariant over the observation interval) so as to maximize the a posteriori probability $p(\theta|r(t))$.² Since the unknown phase θ can be assumed uniformly distributed in the interval $(-\pi, \pi)$, equivalently we can maximize the conditional probability $p(r(t)|\theta)$. For the assumed additive white Gaussian noise channel model assumed, this probability takes the well-known form

$$p(r(t)|\theta) = \overline{p(r(t)|\theta, \{a_k\}, \{b_k\})}^{I, Q} \quad (3)$$

where the overbar denotes statistical averaging over the I and Q data sequences and

$$p(r(t)|\theta, \{a_k\}, \{b_k\}) = C \exp\left\{-\frac{2}{N_0} \int_{T_d}^{T_d+\gamma T} r(t) s(t, \theta) dt\right\} \times \exp\left\{-\frac{1}{N_0} \int_{T_d}^{T_d+\gamma T} s^2(t, \theta) dt\right\} \quad (4)$$

where C is an arbitrary constant (that includes the parameter independent term $\exp\left\{-\frac{1}{N_0} \int_{T_d}^{T_d+\gamma T} r^2(t) dt\right\}$) and $T_d \triangleq (N_d + \delta)T$ (N_d integer) denotes the inherent delay introduced by the pulse-spread filter $h(t)$.³ Without any loss in generality, we now assume that the pulse shape $p(t)$ is truncated such that the significant ISI results only from K past symbols. Equivalently, the duration of the pulse $p(t)$ is limited to a maximum duration of $(K+1)T$ sec.

In the case of zero ISI, the second exponential factor in (4), i.e., that corresponding to the signal energy, will be constant and independent of the I and Q data sequences $\{a_k\}, \{b_k\}$ and thus (4) would simplify to⁴

$$p(r(t)|\theta, \{a_k\}, \{b_k\}) = C \exp\left\{-\frac{2}{N_0} \int_{T_d}^{T_d+\gamma T} r(t) (1, 0 \theta) dt\right\} \quad (5)$$

Unfortunately, in the ISI case the signal energy exponential factor depends on the I and Q data sequences and thus for evaluation of the true MAP estimate of phase it should not be ignored.⁵ For the uniform case however, let us proceed by ignoring

²For convenience, we shall assume that γ is integer, i.e., the observation interval corresponds to an integer number of baud intervals. This is typical of MAP estimation problems of this type.

³In practice, T_d would be determined by the symbol synchronizer employed in the receiver.

⁴Herein, we continue to use "C" to denote an arbitrary constant despite the fact that its value may vary from usage to usage.

this factor (as was done in [4]) with an aim towards simplicity of implementation at the same time however, understanding, however, that the resulting Structures will not necessarily be optimum⁶.

Substituting (1) together with (2) into (5) and simplifying results in

$$p(r(t)|\theta, \{a_k\}, \{b_k\}) = C \prod_{i=-(N_d+\gamma)}^A \exp\{a_i I_c(i, \theta)\} \times \prod_{i=-(N_d+\gamma)}^K \exp\{b_i I_s(i, \theta)\} \quad (6)$$

where

$$I_c(i, \theta) \triangleq \frac{2\sqrt{2P}}{N_0} \int_{T_d}^{T_d+\gamma} r(t) \cos(\omega_c t + \theta) p(t + iT) dt \quad (7)$$

$$I_s(i, \theta) \triangleq \frac{2\sqrt{2P}}{N_0} \int_{T_d}^{T_d+\gamma} r(t) \sin(\omega_c t + \theta) p(t + iT) dt$$

Since the independent data sequences $\{a_k\}, \{b_k\}$ are each independent identically distributed (i.i.d.), then averaging over these sequences results in

$$p(r(t)|\theta) = C \prod_{i=-(N_d+\gamma)}^K \cosh\{I_c(i, \theta)\} \times \prod_{i=-(N_d+\gamma)}^K \cosh\{I_s(i, \theta)\} \quad (8)$$

We refer to this as the *partitioned form* of the likelihood function. As we shall see later on, such partitioning is only possible in the ISI case by ignoring the signal energy dependent exponential factor in the likelihood function, i.e., using the form in (5) rather than that in (4).

⁵In [4], for the purpose of simplicity of implementation (and also analysis), this signal energy dependent factor was ignored in deriving the MAP estimate. Thus the MAP estimate of carrier phase derived there and the closed structures motivated by it are not strictly speaking "optimum" (in the MAP estimation sense). Nevertheless, we shall show later on that these practical implementable structures do indeed achieve excellent performance despite their inherent suboptimality when compared to the conventional schemes that completely ignore ISI in their design.

⁶Herein, when describing a structure, we use the word *optimum* without quotation marks to mean a closed loop structure that is motivated by the MAP estimation approach in that the error signal in the loop is derived from the derivative of the likelihood function (or a monotonic function of it) with respect to the unknown parameter, θ . This is consistent with similar usage in the literature regarding the derivation of tracking loops derived from open loop MAP parameter estimation.

In view of the partitioned form of the likelihood function in (8), it is advantageous to take the logarithm of this function before maximizing it with respect to the unknown phase parameter, θ . Doing so gives

$$\ln p(r(t)|\theta) = \ln C + \sum_{i=(N_s+\gamma)}^K \ln \cosh\{I_c(i, \theta)\} + \sum_{i=(N_s+\gamma)}^K \ln \cosh\{I_s(i, \theta)\} \triangleq \ln C + A(\theta) \quad (9)$$

Differentiating (9) with respect to θ provides the error signal (actually the negative of the error signal) for the closed loop phase tracking structure motivated by the approximate MAP approach described above. Thus,

$$-\frac{\partial \ln p(r(t)|\theta)}{\partial \theta} \triangleq e(\theta) = \sum_{i=(N_s+\gamma)}^K \int (i\theta) \tanh\{I_c(i, \theta)\} I_c(i, \theta) \tanh\{I_s(i, \theta)\} \quad (10)$$

The interpretation of (9) is that a closed loop structure using (9) to characterize its error signal is the *superposition* of $K + N_s + \gamma + 1$ I-Q loops each operating over a different portion of the pulse response $I_c(f)$. Also, the composite loop is assumed to update itself every T sec as is the case for the conventional (zero ISI) I-Q loop. For the special case of BPSK modulation, the terms in the second I-Q summation in (10) are all zero. One implementation of a BPSK loop based on (10) is illustrated in Fig. 2 where the hyperbolic tangent function has been omitted which is valid for small values of its argument.⁷ In keeping with previous nomenclature, such a loop will be referred to in this paper as an *ISI-compensated I-Q loop*.

3. Performance of the BPSK ISI-Compensated I-Q Loop

3.1 The Stochastic Differential Equation of Operation

In this section, we first derive the stochastic differential equation of operation of the ISI-compensated I-Q loop of Fig. 2 and then compute its mean-squared phase jitter.

As previously mentioned, the signal $r(t)$ at the input to the receiver is composed of the sum of the signal $s(t, \theta)$ and a bandlimited white Gaussian noise process which

⁷In practice, when designing closed loop structures based on the above, it is customary to approximate the hyperbolic tangent nonlinearity by its small and large argument approximations, namely, $\tanh x \cong x$ for small x and $\tanh x \cong \text{sgn } x$ for large x . Such approximations, respectively, lead to small and large signal-to-noise ratio (SNR) tracking structures.

can be expressed in the form

$$n(t) = \sqrt{2} [N_c(t) \cos(\omega_c t + \theta) - N_s(t) \sin(\omega_c t + \theta)] \quad (11)$$

where $N_c(t), N_s(t)$ are independent low pass white Gaussian noise processes with single-sided power spectral density N_0 watts/Hz. For BPSK we can express the signal as $s(t, \theta) = \sqrt{2P} m(t) \sin(\omega_c t + \theta)$. Demodulating $r(t)$ with the quadrature reference signals $r_c(t) = \sqrt{2} \cos(\omega_c t + \hat{\theta})$ and $r_s(t) = \sqrt{2} \sin(\omega_c t + \hat{\theta})$ produces (ignoring second order harmonics of the carrier) the quadrature phase detector outputs

$$\begin{aligned} \varepsilon_c(t) &= [\sqrt{P} m(t) - N_s(t)] \sin \phi + N_c(t) \cos \phi \\ \varepsilon_s(t) &= [\sqrt{P} m(t) - N_s(t)] \cos \phi - N_c(t) \sin \phi \end{aligned} \quad (12)$$

where $\phi \triangleq \theta - \hat{\theta}$ denotes the phase error in the loop. Weighting these signals by $p(t + iT)$ and integrating over the observation time interval gives the pair of signals $z_{c,i}(t), z_{s,i}(t)$ which when multiplied result in the component of the total error signal contributed by the i th loop. Assuming a modulation $m(t)$ of the form of $m_j(t)$ in (2), these signals take the form⁸

$$\begin{aligned} z_{c,i}(t) &= \int_{T_d}^{T_d + \gamma} \varepsilon_c(t) p(t + iT) dt = \sqrt{PT} \left| \sum_{j=1}^A a_j I_{j,i} \right| \sin \phi - N_{s,i} \sin \phi + N_{c,i} \cos \phi \\ z_{s,i}(t) &= \int_{T_d}^{T_d + \gamma} \varepsilon_s(t) p(t + iT) dt = \sqrt{PT} \left| \sum_{j=1}^A a_j I_{j,i} \right| \cos \phi - N_{s,i} \cos \phi - N_{c,i} \sin \phi \end{aligned} \quad (13)$$

where $N_{s,i}, N_{c,i}$ are zero mean Gaussian random variables defined by

$$N_{s,i} = \int_{T_d}^{T_d + \gamma} N_s(t) p(t + iT) dt, \quad N_{c,i} = \int_{T_d}^{T_d + \gamma} N_c(t) p(t + iT) dt \quad (14)$$

and the $I_{i,j}$'s are ISI parameters defined by

$$I_{i,j} = \frac{1}{T} \int_{T_d}^{T_d + \gamma} p(t + iT) p(t + jT) dt = I_j \quad (15)$$

The variances of $N_{s,i}, N_{c,i}$ are easily computed as

$$\text{var}\{N_{s,i}\} = \text{var}\{N_{c,i}\} = \frac{N_0 T}{2} I_{i,i} \quad (16)$$

The noise samples from different loops are correlated with correlation coefficients

⁸We can ignore the weighting of the integrators by the factor $2\sqrt{2P}/N_0$ since for this implementation this gain will eventually be absorbed in the total loop gain.

$$E\{N_{c,i}N_{c,j}\} = E\{N_{s,i}N_{s,j}\} = \frac{N_0 T}{2} I_{i,j} \quad (16)$$

However, the $N_{c,i}$'s and the $N_{s,j}$'s are independent for all i and j .

Multiplying $z_{c,i}(t)$ and $z_{s,i}(t)$ produces the error signal in the i th loop, namely,

$$\begin{aligned} z_i(t) = z_{c,i}(t)z_{s,i}(t) = \sin 2\phi \left[\frac{PT^2}{2} \left(\sum_{j=(N_d+\gamma)}^K a_{-j} I_{j,i} \right)^2 - \sqrt{PT} N_{s,i} \left(\sum_{j=(N_d+\gamma)}^K a_{-j} I_{j,i} \right) + \frac{N_{s,i}^2}{2} - \frac{N_{c,i}^2}{2} \right] \\ - i \cos 2\phi \left[\sqrt{PT} \left(\sum_{j=(N_d+\gamma)}^K a_{-j} I_{j,i} \right) - N_{s,i} \right] N_{c,i} \end{aligned} \quad (17)$$

Finally, the dynamic error signal of the composite of all loops is

$$z(t) = \sum_{i=(N_d+\gamma)}^K z_i(t) \quad (18)$$

and (assuming $d\theta/dt = 0$) the stochastic differential equation of loop operation is given by

$$2p\phi + PT^2 KF(p) \sin 2\phi \left[\sum_{i=(N_d+\gamma)}^K \left(\sum_{j=(N_d+\gamma)}^K a_{-j} I_{j,i} \right)^2 \right] = KF(p) N_e(t, 2\phi) \quad (19)$$

where p denotes the Heaviside operator, K is the total open loop gain, $F(p)$ is the loop filter transfer function, and $N_e(t, 2\phi)$ is the equivalent additive noise defined by

$$\begin{aligned} N_e(t, 2\phi) = \sin 2\phi \sum_{i=(N_d+\gamma)}^K \left[N_{c,i}^2 - N_{s,i}^2 - I 2 \sqrt{PT} N_{s,i} \sum_{j=(N_d+\gamma)}^K a_{-j} I_{j,i} \right] \\ + \cos 2\phi \sum_{i=(N_d+\gamma)}^K \left[2N_{c,i} \left(\sum_{j=(N_d+\gamma)}^K a_{-j} I_{j,i} \right) - N_{s,i} \sqrt{PT} \sum_{j=(N_d+\gamma)}^K a_{-j} I_{j,i} \right] \end{aligned} \quad (20)$$

and is a piecewise constant (over intervals of T sec) random process. As in analyses of BPSK I-Q and Costas loops without ISI we rewrite the second term on the left hand side of (19) in terms of its statistical mean and the variation around this mean. The statistical mean represents the so-called *loop S-curve* and variation around the mean is the *loop self noise*. Since the variance of the zero mean self noise is proportional (for the BPSK case considered here) to $\sin^2 2\phi$, it yields a negligible

contribution to the overall mean-squared phase jitter in the SNR region of typical interest. Thus, as has been done in previous analyses of this type, we shall ignore its presence and replace the second term on the right hand side of (19) by simply its statistical mean. Doing this and at the same time linearizing the loop (i.e., replacing $\sin 2\phi$ by 2ϕ) gives the linear loop equation of operation, namely,⁹

$$2\phi = \frac{KF(p)N_e(t,0)}{p + PT^2KF(p)E\left\{\sum_{i=-(N_d+\gamma)}^K \left(\sum_{j=-(N_d+\gamma)}^K a_j I_{j,i}\right)^2\right\}} H_{\gamma\phi}(p) \frac{N_e(t,0)}{PT^2E\left\{\sum_{i=-(N_d+\gamma)}^K \left(\sum_{j=-(N_d+\gamma)}^K a_j I_{j,i}\right)^2\right\}} \quad (21)$$

where $H_{\gamma\phi}(p)$ is the closed loop transfer function for the BPSK ISI-compensated I-Q loop.

3.2 The Mean-Squared Phase Jitter Performance

Following the approach taken in [23], the mean-squared phase jitter is easily derived from (23) as

$$\sigma_{2\phi}^2 = \frac{N_E B_L}{P^2 T^4 \left[E \left\{ \sum_{i=-(N_d+\gamma)}^K \left(\sum_{j=-(N_d+\gamma)}^K a_j I_{j,i} \right)^2 \right\} \right]^2} \quad (22)$$

where B_L denotes the loop bandwidth (obtained from the magnitude of the closed loop transfer function) and N_E is the flat single-sided power spectral density of the equivalent noise process $N_e(t,0)$ which can be modeled as a delta-correlated process [2,3] with autocorrelation function $R_{N_e}(\tau) = E\{N_e(t,0)N_e(t-\tau,0)\}$. Thus,

$$N_E = 2 \int_0^\infty R_{N_e}(\tau) d\tau \quad (23)$$

The squared expectation in the denominator of (22) represents the signal \times signal ($S \times S$) term in the loop error signal. It can be evaluated as

$$\left[E \left\{ \sum_{i=-(N_d+\gamma)}^K \left(\sum_{j=-(N_d+\gamma)}^K a_j I_{j,i} \right)^2 \right\} \right]^2 = \left[\sum_{i=-(N_d+\gamma)}^K \sum_{j=-(N_d+\gamma)}^K I_{i,j}^2 \right]^2 \quad (24)$$

⁹For the equivalent noise term we may let $\phi = 0$ without any loss in generality.

Substituting (24) into (22) gives

$$\sigma_{\gamma\phi}^2 = \frac{N_e B_L}{P^2 T^4} \left[\sum_{i=-(N_d+\gamma)}^K \sum_{j=-(N_d+\gamma)}^K I_{i,j}^2 \right] = \frac{4N_0 B_L}{P^2 S_L} \quad (25)$$

where

$$S_L \triangleq \left[\sum_{i=-(N_d+\gamma)}^K \sum_{j=-(N_d+\gamma)}^K I_{i,j}^2 \right]^2 \times \left(\frac{N_L}{4PN_0 T^2} \right)^2 \quad (26)$$

is the so-called *squaring loss* associated with the loop. We now proceed to evaluate the denominator of (2.6).

From (20), we have

$$N_e(t, 0) = 2 \sum_{i=-(N_d+\gamma)}^K N_{c,i} N_{s,i} \sqrt{PT} \left[\sum_{j=-(N_d+\gamma)}^K a_{-j} I_{j,i} \right]; \quad T_d + \gamma T \leq t \leq T_d + (\gamma + 1)T \quad (27)$$

with a variance (see Appendix A) given by

$$\sigma_N^2 = \sum_{i=-(N_d+\gamma)}^K \sum_{j=-(N_d+\gamma)}^K \left[N_0^2 T^2 I_{i,j}^2 + 2PN_0 T \sum_{k=-(N_d+\gamma)}^K I_{i,k} I_{j,k} \right] \quad (28)$$

which is independent of t . To compute the autocorrelation of $N_e(t, 0)$ we must model this piecewise constant random process in an arbitrary T -sec time interval, e.g., $T_d + (\gamma + m)T \leq t \leq T_d + (\gamma + m + 1)T$ with m integer. In particular,

$$N_e(t, 0) = 2 \sum_{i=-(N_d+\gamma+m)}^{K-m} N_{c,i}(m) N_{s,i}(m) \sqrt{PT} \left[\sum_{j=-(N_d+\gamma+m)}^{K-m} a_{-j} I_{j,i}(m) \right]; \quad N(m) \quad (29)$$

where

$$N_{c,i}(m) \triangleq \int_{T_d+mT}^{T_d+(\gamma+m)T} N_c(t) p(t+iT) dt; \quad N_s(m) \triangleq \int_{T_d+mT}^{T_d+(\gamma+m)T} N_s(t) p(t+iT) dt \quad (30)$$

$$I_{i,j}(m) \triangleq \frac{1}{T} \int_{T_d+mT}^{T_d+(\gamma+m)T} p(t+iT) p(t+jT) dt \triangleq I_{j,i}(m)$$

Since for a piecewise constant random process, the autocorrelation function will be piecewise linear (see Fig. 3), it is sufficient to compute the values of $R_{N_e}(\tau)$ at integer multiples of T , namely, $R_{N_e}(nT) = E\{N(0)N(n)\} \triangleq R(n)$ where $R(0) = E\{N^2(0)\} = \sigma_{N_e}^2$ as previously given in (31). Furthermore, since $R_{N_e}(\tau)$ extends only from $-\gamma T$ to γT ,

then from (23) we have

$$N_E = 2T \left[\alpha + 2 \sum_{n=1}^{\gamma-1} R(n) \right] + 4T \sum_{n=1}^{\gamma-1} R(n) \quad (31)$$

The evaluation of $\{R(n); n = 1, 2, \dots, \gamma-1\}$ is carried out in Appendix A with the result

$$R(n) = \sum_{i=-(N_d+\gamma)}^K \sum_{j=-(N_d+\gamma+n)}^{K-n} \left[N_0^2 T^{-2} I_{i,j}(0) + 2PN_0 T^3 J_{i,j}(n) \sum_{k=(N_d+\gamma)}^{K-n} I_{i,k}(0) I_{j,k}(n) \right] \quad (32)$$

where

$$J_{i,j}(m) \triangleq \frac{1}{T} \int_{T_d}^{T_d+\gamma T} p(t+iT) p(t+jT) dt \quad (33)$$

Note that $J_{i,j}(m)$ differs from $I_{i,j}(m)$ of (30) in that the upper limit is $T_d + \gamma T$ rather than $T_d + (\gamma + m)T$. Also note that $I_{i,j}(0) = J_{i,j}(0) = I_{i,j}$, and $I_{i,j}(n) = I_{i+n,j+n}$ where $I_{i,j}$ was previously defined in (15). Making these substitutions in (32) we see that for $n = 0$ this equation reduces to (28) as it should. Finally, substituting (28) and (33) in (31) and then dividing by $4PN_0 T^4$ we get

$$\frac{N_E}{4PN_0 T^4} = \alpha + \frac{\beta}{2R_d} \quad (34)$$

where $R_d = PT/N_0$ denotes the SNR and

$$\begin{aligned} \alpha &= \sum_{i=-(N_d+\gamma)}^K \sum_{j=-(N_d+\gamma)}^K I_{i,j} \sum_{k=-(N_d+\gamma)}^K J_{i,j} I_{j,k} + 2 \sum_{n=1}^{\gamma-1} \sum_{i=-(N_d+\gamma)}^K \sum_{j=-(N_d+\gamma+n)}^{K-n} J_{i,j}(n) \sum_{k=(N_d+\gamma)}^{K-n} I_{i,k} I_{j+n,k+n} \\ \beta &= \sum_{i=-(N_d+\gamma)}^K \sum_{j=-(N_d+\gamma+n)}^{K-n} I_{i,j}^2 + 2 \sum_{n=1}^{\gamma-1} \sum_{i=-(N_d+\gamma)}^K \sum_{j=-(N_d+\gamma+n)}^{K-n} J_{i,j}^2(n) \end{aligned} \quad (35)$$

The quantity “ α ” in (35) represents the signal \times noise (S \times A) term in the loop error signal whereas the quantity “ $\beta/2R_d$ ” represents the noise \times noise (N \times N) term in this same signal. Substituting (34) into (26) gives the final desired form for the squaring loss, namely,

$$S_L = \frac{\left[\sum_{i=-(N_d+\gamma)}^K \sum_{j=-(N_d+\gamma)}^K I_{i,j}^2 \right]^2}{\alpha + \frac{\beta}{2R_d}} \quad (36)$$

For zero ISI, e.g., $p(t)$ a rectangular pulse, we have that $\gamma = 1$, $N_d = 0$, $K = 0$ and

$I_{i,j} = 0, i \neq j, I_{i,i} = 1, J_{i,j} = 0, i \neq j, J_{i,i} = 1$. Thus, $\alpha = \beta = 1$ and (39) simplifies to

$$S_L = \frac{2R_d}{1+2R_d} \quad (37)$$

which is a well-known result for the conventional (wideband) I-Q loop with zero ISI [2]. By analogy, for a one-symbol observation in the ISI environment, i.e., $y = 1$, (36) simplifies to

$$S_L = \frac{\left[\sum_{i=-(N_d+1)}^K \sum_{j=-(N_d+1)}^K I_{i,i}^2 \right]}{\sum_{i=-(N_d+1)}^K \sum_{j=-(N_d+1)}^K \sum_{k=-(N_d+1)}^K I_{i,j} I_{j,k} I_{k,i} + \frac{\sum_{i=-(N_d+1)}^K \sum_{j=-(N_d+1)}^K I_{i,j}^2}{2R_d}} \quad (38)$$

To assess the benefit obtained by using the ISI-compensated I-Q loop rather than the conventional (wideband) I-Q, we must now determine the performance of the latter in the ISI environment.

4. Mean-Squared Phase Jitter Performance of the Conventional I-Q Loop in an ISI Environment

The conventional I-Q loop is illustrated in Fig. 4. The performance of this loop in an ISI environment such as that modeled in this paper has been previously obtained [4,7]. In particular, the squaring loss is given by [7]

$$S_L = \frac{\left[\sum_{j=-(N_d+1)}^K I_j^2 \right]^2}{\sum_{j=-(N_d+1)}^K I_j^2 + \frac{1}{2R_d}} \quad (39)$$

where

$$I_j = \frac{1}{T} \int_{T_d}^{T_d+T} p(t+jT) dt \quad (40)$$

We observe that the ISI-contaminated pulse shape has no bearing on the $N \times N$ term in the denominator of (39) as one would anticipate. (Note from (26) that this is not

¹⁰In [5], the delay of the filter was not explicitly accounted for. However, it is a simple matter to modify the results obtained there to include this parameter.

true for the ISI-compensated loop with $\gamma = 1$.) Also, the $S \times S$ term (the numerator of (40)) is equal to the square of the $S \times N$ term.

5. Numerical Examples

To illustrate the behavior of the ISI compensated I-Q loop, we consider an N -pole Butterworth filter for the pulse spreading filter $h(t)$. This results in the pulse response $p(t) = g(t) * h(t)$ ($g(t)$ a unit power rectangular pulse) given by

$$p(t) = 2 \operatorname{Re} \left\{ \int_0^\infty T \frac{\sin \pi f T}{\pi f T} H_N(f) e^{j 2\pi f t} df \right\} \quad (41)$$

where

$$H_N(f) = \left[+ \sum_{n=1}^N c_n j^n (f / f_0)^n \right] \quad ; \quad c_N = 1 \quad (42)$$

with f_0 the 3 dB frequency. For a given value of N , the filter coefficients $\{c_n\}$ can be found in any standard textbook on filter theory. An abbreviated table of these values for $N = 1, 2, 3, 4$, and 5 is given in Table 1. Fig. 5 is a plot of the response for $f_0 T = 1$ and $N = 5$. Figs. 6a,b are plots of S_1 as determined from (38) versus R_d in dB for observations $\gamma = 1, 2$, and 3 baud intervals and two different values of T_d namely, $T_d = 0.25$ ($N_d = 0, \delta T = 0.25$) and $T_d = 0.50$ ($N_d = 0, \delta T = 0.50$). The first of the two values of T_d is indicative of the delay of the pulse $p(t)$ whereas the second is indicative of a value that places the peak of the pulse in the middle of the observation interval for $\gamma = 1$. For comparison, the performances of the conventional loop with zero ISI and in the above ISI environment as determined from (37) and (39), respectively, are also illustrated. In both cases, we observe that a reasonable improvement in performance is obtained by using the ISI-compensated I-Q loop as opposed to the conventional I-Q loop, particularly, as γ approaches K , i.e., the observation interval extends over all the ISI.

6. The MAP Estimation of Carrier Phase Revisited

We return to the initial problem of finding the MAP estimate of carrier phase in an ISI environment, now, however, maintaining the dependence of the likelihood

function on the ISI-dependent signal energy term that was heretofore ignored. Substituting (1) and (2) into now (4) (rather than (5)) gives after simplification ¹

$$\begin{aligned}
 p(r(t)|\theta, \{a_k\}, \{b_k\}) = & C \prod_{i=(N_d+1)}^K \exp\{a_{-i} I_i(i, \theta)\} \times \prod_{j=(N_d+1)}^K \prod_{k=(N_d+1)}^K \exp\left\{-\frac{2PT}{N_0} a_{-j} a_k I_{j,k}\right\} \\
 & \times \prod_{i=(N_d+1)}^K \exp\{b_{-i} I_i(i, \theta)\} \times \prod_{j=(N_d+1)}^K \prod_{k=(N_d+1)}^K \exp\left\{-\frac{2PT}{N_0} b_{-j} b_k I_{j,k}\right\}
 \end{aligned} \tag{43}$$

We note that that because the signal energy exponential factor involves the square of the transmitted signal $s(t, \theta)$ as an integrand and there exists *pairwise dependence* on on the elements of the data sequences. This prevents the averaging over the data sequences from producing a partitioned form of the likelihood function as was obtained in (8). Thus, it will not be convenient to take the logarithm of the likelihood ratio prior to differentiating it with respect to the unknown parameter θ instead we proceed as follows

Restricting our attention to the BPSK case, we arrange the i th data sequence $\{a_k^{(i)}, i = 1, 2, \dots, 2^{K+N_d+2}\}$ and sequence of translated pulse shapes $\{p(t - iT)\}$ in the form of vectors, and describe the pairwise intersymbol interferences by a matrix, namely,

$$\begin{aligned}
 \mathbf{a}^{(i)T} &= [a_{-K}^{(i)}, \dots, a_{-1}^{(i)}, a_0^{(i)}, a_1^{(i)}, \dots, a_{N_d}^{(i)}, a_{N_d+1}^{(i)}] \\
 \mathbf{p}(t)^T &= [p(t + KT), \dots, p(t + T), p(t), p(t - T), \dots, p(t - (N_d + 1)T)] \\
 I &= [I_{i,j}]
 \end{aligned} \tag{44}$$

Then, corresponding to the i th data sequence, define the i th effective pulse shape $p_i(t), i = 1, 2, \dots, 2^{K+N_d+2}$ by

$$p_i(t) = \mathbf{a}^{(i)T} \mathbf{p}(t) \tag{45}$$

In terms of this vector and matrix representation, we can write the average of (47)

¹¹For simplicity, we shall consider only the case of a single baud interval observation ($\gamma = 1$) since as we shall see this is sufficient to justify the points that need to be made.

over the data sequence $\{a_k\}$ as

$$p(r(t)|\theta) = C \sum_{i=1}^{2^{K+N_d+2}} \exp(-2R_d w_i) \times \exp(I_c'(i, \theta)) \quad (46)$$

where

$$w_i = \mathbf{a}^{(i)T} \mathbf{I} \mathbf{a}^{(i)}, \quad I_c'(i, \theta) \triangleq \frac{2\sqrt{2P}}{N_0} \int_{t_d}^{t_d+T} r(t) \cos(\omega_c t - \theta) p_i(t) dt \quad (47)$$

Note the difference between $I_c'(i, \theta)$ of (51) and $I_c(i, \theta)$ of (7), namely, the former folds all the ISI for the i th sequence into the integration interval in terms of $p_i(t)$

whereas the latter only involves only the ISI for a single translate, e.g., $p(t + iT)$, of the pulse response. We refer to (46) as the *unpartitioned form* of the likelihood

function. Differentiating (46) with respect to θ provides an error signal (actually the negative of the error signal) for a closed loop tracking structure motivated by the true MAP approach described above. In particular,

$$-\frac{\partial p(r(t)|\theta)}{\partial \theta} \triangleq e(\theta) = C \sum_{i=1}^{2^{K+N_d+2}} \exp(-2R_d w_i) \times I_s'(i, \theta) \exp(I_c'(i, \theta)) \quad (48)$$

where by analogy with (51)

$$I_s'(i, \theta) \triangleq \frac{2\sqrt{2P}}{N_0} \int_{t_d}^{t_d+T} r(t) \sin(\omega_c t - \theta) p_i(t) dt \quad (49)$$

An implementation of a BPSK tracking loop with an error signal based on (48) is illustrated in Fig. 7. Note that the complexity of this implementation in terms of the number of superimposed loops needed to form the composite error signal is *exponentially* dependent on the length of the sequence i.e., 2^{K+N_d+2} as opposed to being *linearly* dependent on sequence length for the structure based on the partitioned form of the likelihood function (see Fig. 2).

The result in (52) can be slightly simplified by noting in (50) that for any given data sequence the weight w_i will be identical for both the data sequence and its complement. On the other hand, for this same pair of sequences, the second exponential factor in (50) has equal and opposite exponents. Thus, for a given data sequence and its complement, these two terms can be combined into a hyperbolic

cosine function of $I_c(i, \theta)$ with the signal energy dependent exponential factor $\exp(-2R_d w_i)$ as a weighting coefficient. When this is done, then differentiation with respect to θ gives the alternate form

$$-\frac{\partial p(r(t)|\theta)}{\partial \theta} \triangleq e(\theta) = C \sum_{i=1}^{2^{K+N_d+1}} \exp(-2R_d w_i) I_s(i, \theta) \sinh(I_c(i, \theta)) \quad (50)$$

where the sum ranges over only those sequences with $a_0 = 1$, i.e., half the total number of sequences.

Suppose now that analogous to what was done previously in this paper, one linearizes the loop in Fig. 7, i.e., remove the hyperbolic sine nonlinearity which is valid for small SNR. Then, (50) reduces to

$$-\frac{\partial p(r(t)|\theta)}{\partial \theta} \triangleq e(\theta) = C \sum_{i=1}^{2^{K+N_d+1}} \exp(-2R_d w_i) I_s(i, \theta) I_c(i, \theta) \quad (51)$$

which suggests an ISI-compensated I-Q loop in the form of a superposition of weighted low SNR I-Q loops. The stochastic differential equation of operation and performance of such a loop can be obtained in a manner analogous to the approach taken in Section 3. In particular, it is straightforward to show that analogous to (19), the loop equation of operation is given by

$$2p\phi + PT^2KF(p)\sin 2\phi \left[\sum_{i=1}^{2^{K+N_d+1}} \exp(-2R_d w_i) \left(\sum_{j=(N_d+1)}^K a_j I_{j,i} \right)^2 \right] = KF(p)N_c^i(t, 2\phi) \quad (52)$$

where somewhat analogous to (15)

$$I_{j,i} \triangleq \frac{1}{T} \int_{T_d}^{T_d+T} p(t+jT) p_i(t) dt \neq I_{i,j} \quad (53)$$

and

$$\begin{aligned} N_c^i(t, 2\phi) = & \sin 2\phi \sum_{i=1}^{2^{K+N_d+1}} \exp(-2R_d w_i) \left[N_{c,i}^2 - N_{s,i}^2 + 2\sqrt{PT} N_{s,i} \left(\sum_{j=(N_d+1)}^K a_j I_{j,i} \right) \right] \\ & + \cos 2\phi \sum_{i=1}^{2^{K+N_d+1}} 2 \exp(-2R_d w_i) N_{c,i} \left[N_{s,i} - \sqrt{PT} \left(\sum_{j=(N_d+1)}^K a_j I_{j,i} \right) \right] \end{aligned} \quad (54)$$

In (54), $N_{c,i}^i$ and $N_{s,i}^i$ are zero mean Gaussian random variables defined by

$$N_{s,i}^i = \int_{T_d}^{T_d+T} N_s(t) p_i(t) dt, \quad N_{c,i}^i = \int_{T_d}^{T_d+T} N_c(t) p_i(t) dt \quad (55)$$

with second order correlation properties

$$\text{var}\{N'_{c,i}\} = \text{var}\{N'_{s,i}\} = \frac{N_0 T}{2} J_{i,i}, \quad E\{N'_{c,i} N'_{c,j}\} = E\{N'_{s,i} N'_{s,j}\} = \frac{N_0 T}{2} J_{i,j} \quad (56)$$

where

$$J_{i,j} = \frac{1}{T} \int_{T_d}^{T_d+T} p_j(t) p_i(t) dt = J_{j,i} \quad (57)$$

Ignoring self noise, the mean-squared phase jitter is given by

$$\sigma_{\phi}^2 = \frac{N'_E B_I}{P^2 T^4 \left[E \left\{ \sum_{i=1}^{2^{K+N_d+1}} \exp(-2R_d w_i) \left(\sum_{j=\substack{K \\ (N_d+1)}}^K q_{i,j} I_{j,i} \right)^2 \right\} \right]^2} \quad (58)$$

where N'_E is defined analogous to (23) in terms of the autocorrelation function of the noise $N'_c(t, 0)$ obtained from (54) with $\phi = 0$. Following steps analogous to (25)-(34), we arrive at the desired result for the squaring loss, namely,

$$\mathcal{S}_L = \frac{\left[\sum_{i=1}^{2^{K+N_d+1}} \exp(-2R_d w_i) \sum_{j=\substack{K \\ (N_d+1)}}^K I_{j,i}^2 \right]^2}{\sum_{i=1}^{2^{K+N_d+1}} \sum_{j=1}^{2^{K+N_d+1}} \exp\{-2R_d(w_i + w_j)\} J_{i,j} \sum_{k=\substack{K \\ (N_d+1)}}^K J_{k,i} I_{k,j} + \sum_{i=1}^{2^{K+N_d+1}} \sum_{j=1}^{2^{K+N_d+1}} \exp\{-2R_d(w_i + w_j)\} J_{i,j}^2} \quad (59)$$

The numerical results for the squaring loss as computed from (59) corresponding to the same pulse-spreading filter as considered in Section 5 are superimposed on the results already illustrated in Fig. 6a. We observe that at low SNR, the squaring loss obtained from Fig. 7 which is motivated by the true MAP phase estimate is virtually identical to that obtained from Fig. 2 which was motivated by the MAP phase estimate ignoring the ISI-dependent signal energy term in the likelihood function. At the same time we observe that at high SNR, the squaring loss of the loop in Fig. 7 actually degrades and in fact in the limit of infinite SNR, we would find that $\mathcal{S}_L \rightarrow 0$. This is mathematically justified by (63) since in the limit of large SNR the numerator of this equation behaves as $\exp(-4\beta_N R_d)$ whereas in the same limit the denominator behaves as $\exp(-2\beta_D R_d)$ where β_N and β_D are the dominant positive

ISI terms, respectively, in the numerator and denominator. A similar behavior was observed in [1] for the zero case. In particular, when examining the unpartitioned closed loop structure motivated by the MAP estimation of phase approach, it was found that for an observation of length T in the limit of large R_d , the squaring loop has the asymptotic behavior $\exp(-2R_d)$. An explanation of this somewhat unintuitive result is given in [1] (at least for the ISI-free case.) In particular, the linearization of the exponential (or some hyperbolic) nonlinearity as is done in arriving at Fig. 7 from (50) is from a performance standpoint at high SNR quite inferior to the linearization of the hyperbolic tangent nonlinearity as is done in arriving at Fig. 2 from the BPSK form of (10). As a further check on the validity of the above, we computed the performance of Fig. 7 under the assumption that we set the weights $\{w_i\}$ all equal to zero. The squaring loop performance of this structure, i.e., Fig. 7 with the $\exp(-2R_d w_i)$ weights all set equal to unity, became identical to that of Fig. 2, i.e., the performance of suboptimum structure (ignoring the signal energy-dependent term in the likelihood function that motivates the structure) is independent of whether it results from the partitioned or unpartitioned form of the likelihood function.

Conclusion

We have demonstrated a class of suppressed carrier synchronization loops that are motivated by MAP estimation theory and in the presence of ISI outperform the conventional I-Q loop which is designed on the basis of zero ISI (wideband assumption.) Although the loops were conceived by ignoring the signal energy-dependent ISI term in the likelihood function, the low SNR versions of these loops, i.e., those that which contain no nonlinearity in their inphase arm, perform as well or perhaps better than the low SNR version of the loop based on accounting for these signal energy-dependent terms.

Acknowledgement

The authors would like to acknowledge the contribution of Prof. W. C. Lindsey Of the University Of Southern California to [4]

Appendix A

Evaluation of the Autocorrelation Function of the Equivalent Noise Process

Starting with the definition of the equivalent noise $N_e(t, 0)$ given in (30) of the maintext, we obtain the statistical autocorrelation function (evaluated at integer multiples of nT)

$$\begin{aligned}
 R(n) = & E\left\{N_e(t, 0)N_e(t - 1 - nT, 0)\right\} = 4 \sum_{i=-(N_d+\gamma)}^K \sum_{l=-(N_d+\gamma+n)}^{K-n} E\left\{N_{c,i}(0)N_{c,i}(n)N_{s,i}(0)N_{s,i}(n)\right. \\
 & - \sqrt{PT}N_{s,i}(n)\left(\sum_{j=-(N_d+\gamma)}^K a_{-j}I_{j,i}(0)\right) \cdot \sqrt{PT}N_{s,i}(0)\left(\sum_{k=-(N_d+\gamma+n)}^{K-n} a_{-k}I_{k,i}(n)\right) \\
 & \left. + PT^2\left(\sum_{j=-(N_d+\gamma)}^K a_{-j}I_{j,i}(0)\right)\left(\sum_{k=-(N_d+\gamma+n)}^{K-n} a_{-k}I_{k,i}(n)\right)\right\} \quad (A-1)
 \end{aligned}$$

To evaluate the first term in (A-1) we note that

$$E\left\{N_{c,i}(0)N_{c,i}(n)\right\} = E\left\{\int_{T_d}^{T_d+\gamma} N_c(t)p(t+iT)dt \int_{T_d+nT}^{T_d+(\gamma+n)T} N_c(\tau)p(t+iT)dt\right\} = \frac{N_0T}{2} J_{i,i}(n) \quad (A-2)$$

where

$$J_{i,j}(n) = \frac{1}{T} \int_{T_d+nT}^{T_d+\gamma T} p(t+iT)p(t+jT)dt \quad (A-3)$$

Similarly,

$$E\left\{N_{s,i}(0)N_{s,i}(n)\right\} = \frac{N_0T}{2} J_{i,i}(n) \quad (A-4)$$

Thus, the first term in (A-1) becomes

$$4 \sum_{i=-(N_d+\gamma)}^K \sum_{l=-(N_d+\gamma+n)}^{K-n} E\left\{N_{c,i}(0)N_{c,i}(n)\right\} E\left\{N_{s,i}(0)N_{s,i}(n)\right\} = \sum_{i=-(N_d+\gamma)}^K \sum_{l=-(N_d+\gamma+n)}^{K-n} N_0^2 T^2 J_{i,i}^2(n) \quad (A-5)$$

The second and third terms of (A-1) both evaluate to zero since the noise

components $N_{s,i}(0)$ and $N_{s,i}(n)$ are both zero mean. The fourth term of (A-1) also makes use of (A-2) and is evaluated as

$$\begin{aligned}
 4PT^2 \sum_{i=-(N_d+\gamma)}^K \sum_{l=-(N_d+\gamma+n)}^{K-n} E\{N_{c,i}(0)N_{c,i}(n)\} & \left\{ \prod_{j=-(N_d+\gamma)}^K a_{-,j} I_{j,i}(0) \right\} \left(\prod_{k=-(N_d+\gamma+n)}^{K-n} a_{-,k} I_{k,i}(n) \right) \\
 & = 2PN_0T^3 \sum_{i=-(N_d+\gamma)}^K \sum_{l=-(N_d+\gamma+n)}^{K-n} J_{i,l}^2(n) \sum_{j=-(N_d+\gamma)}^{K-n} I_{j,i}(0) I_{j,l}(n)
 \end{aligned} \tag{A-6}$$

Finally, summing (A-5) and (A-6) gives the desired result, namely,

$$R(n) = \sum_{i=-(N_d+\gamma)}^K \sum_{j=-(N_d+\gamma+n)}^{K-n} \left[N_0^2 T^2 J_{i,j}^2(n) + 2PN_0T^3 J_{i,j}(n) \sum_{k=-(N_d+\gamma)}^{K-n} I_{i,k} I_{j,k}(n) \right] \tag{A-7}$$

Letting $n=0$ in (A-7) gives the variance of the equivalent noise process as

$$\sigma_{N_s}^2 = \sum_{i=-(N_d+\gamma)}^K \sum_{j=-(N_d+\gamma)}^K \left[N_0^2 T^2 I_{i,j}^2 + 2PN_0T^3 I_{i,j} \sum_{k=-(N_d+\gamma)}^K I_{i,k} I_{j,k} \right] \tag{A-8}$$

in arriving at (A-7) and (A-8), we have made use of the fact that $J_{i,j}(0) = I_{i,j}(0) = I_{i,j}$ where $I_{i,j}(m)$ is defined in (33) and 1, , is (defined in (15) of the main text.

References

1. M. K. Simon, H. Tsou and S. M. Hinedi, "Closed loop carrier phase synchronization techniques motivated by likelihood functions," Jet Propulsion Laboratory, Pasadena, CA, *TDA Progress Report* 42119, July-September 1994, pp.83-104.
2. W. C. Lindsey and M. K. Simon, "Optimum performance of suppressed carrier Receivers with Costas Loop Tracking," *IEEE Transactions on Communications*, Vol. COM-25, No. 2, February 1977, pp. 215-227.
3. W. C. Lindsey and M. K. Simon, *Telecommunication Systems Engineering*, Prentice-Hall, Inc., Englewood Cliffs, NJ, 1973. Reprinted by Dover Press, New York, NY, 1991.
4. S. M. Hinedi, "Carrier synchronization in bandlimited channels," PhD Dissertation, University of Southern California, 1987.
5. M. A. Davidov, "Intersymbol interference effects on synchronization loops," Ph.D. dissertation, University of Southern California, Los Angeles, CA, January 1981.
6. W. C. Lindsey and M. A. Davidov, "Intersymbol interference effects on BPSK tracking loops," NTC '80 Conference Record, November 30-December 4, 1980, Houston, Texas, pp. 24.7.1-24.7.5
7. S. M. Hinedi and W. C. Lindsey, "Intersymbol interference effects on BPSK and QPSK carrier tracking loops," *IEEE Transactions on Communications*, Vol. 38, No. 10, October 1990, pp. 1670-1676

Table 1

Coefficients for N -pole Butterworth Filter Polynomial

N	c_1	c_2	c_3	c_4	c_5
2	1.4142				
3	2.0000	2.0000			
4	2.6131	3.4142	2.6131		
5	3.2361	5.2361	5.2361	3.2361	

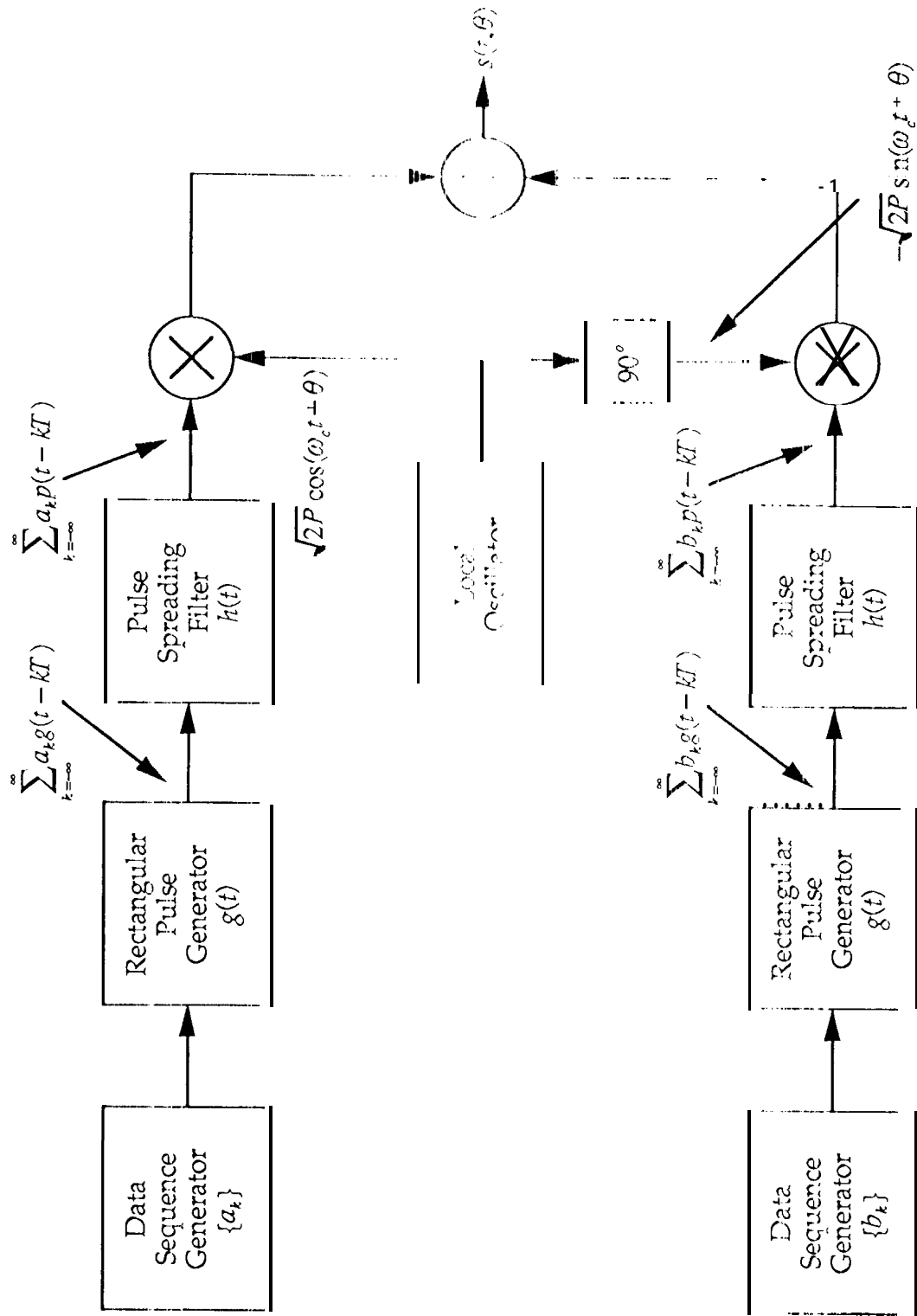


Fig. 1 Digital Communication Transmitter Model

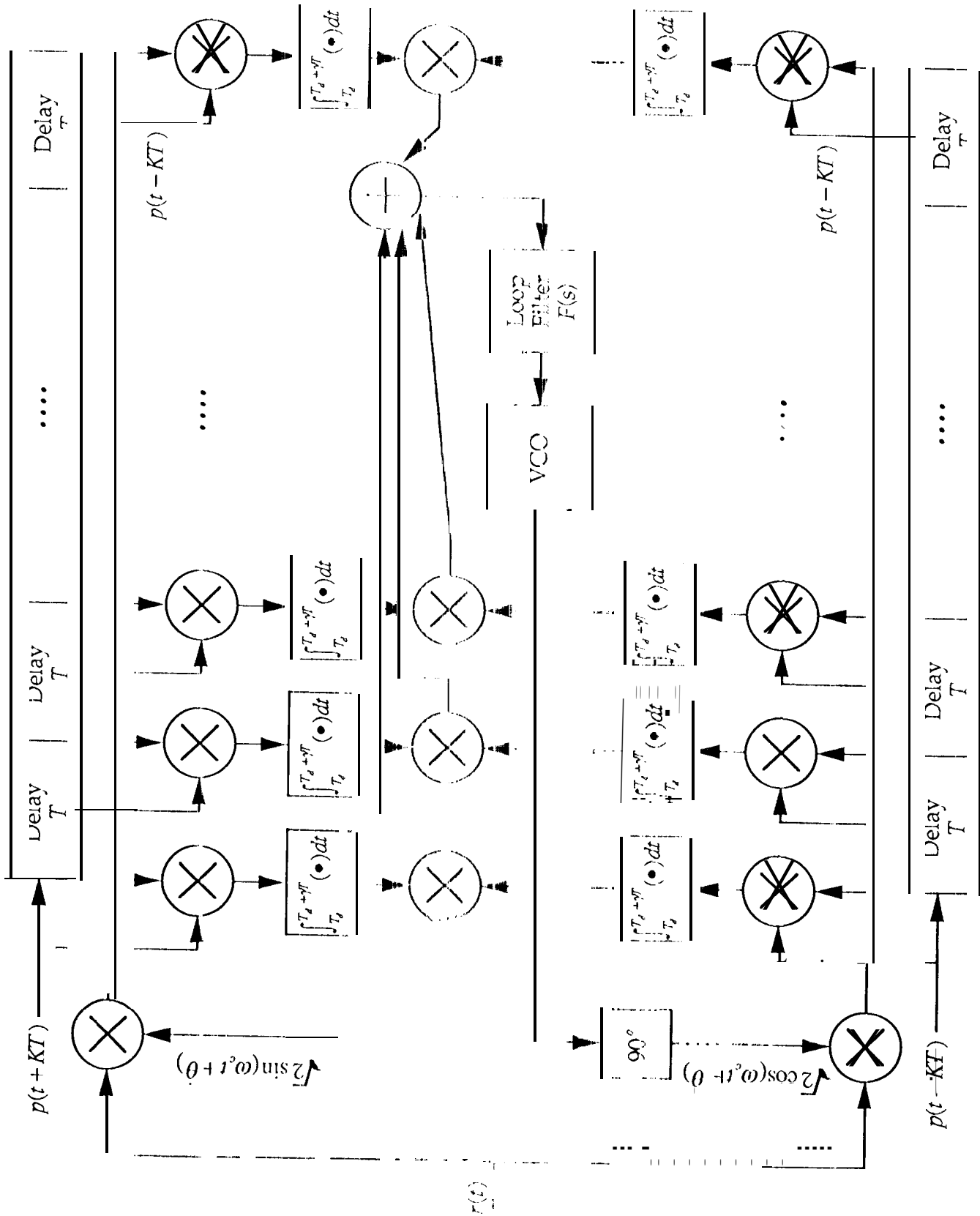


Fig. 2 Block Diagram of Suboptimum (Low SNR) ISI-Compensated I-Q Loop

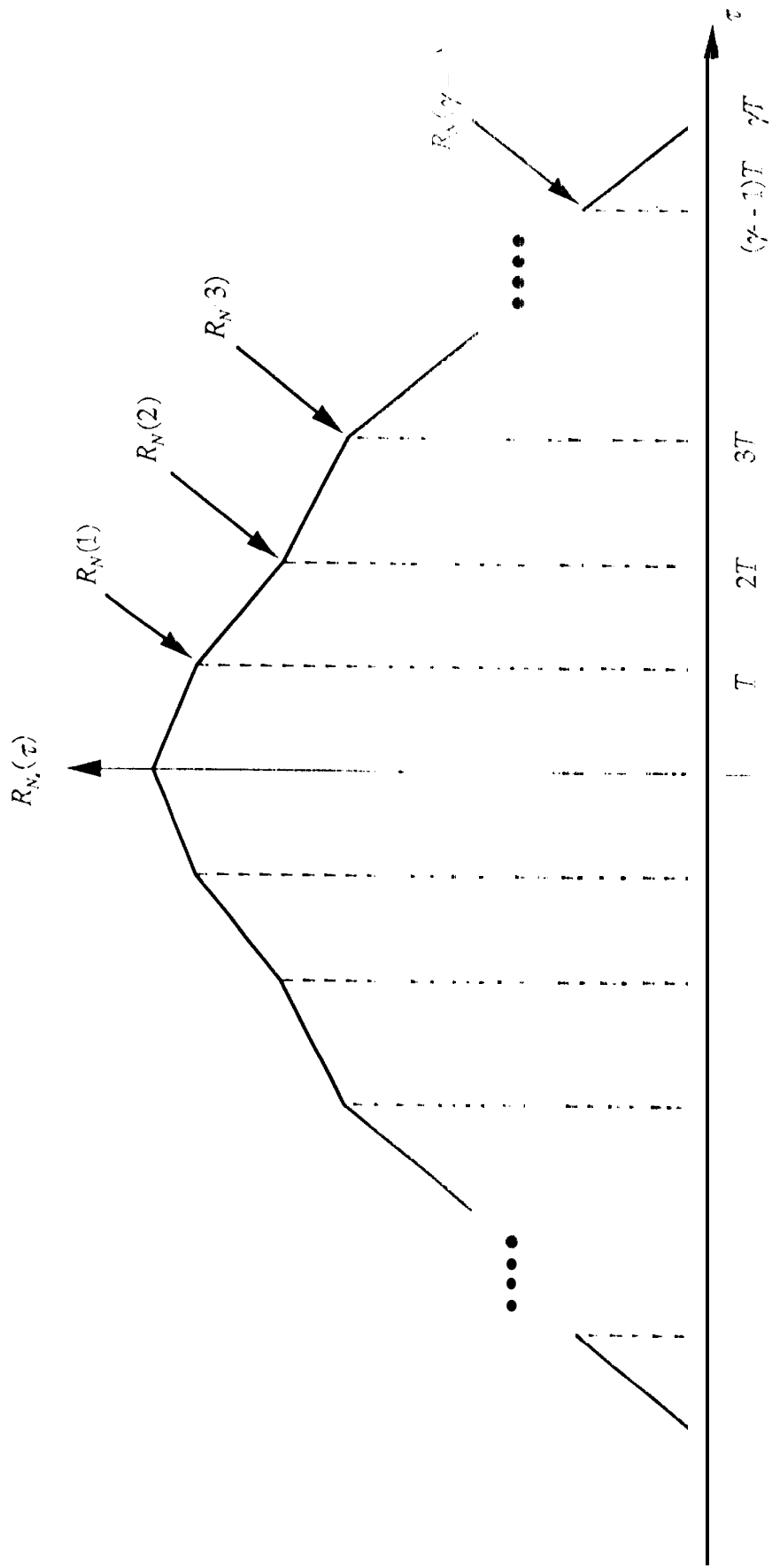


Fig. 3 Autocorrelation function of equivalent noise process

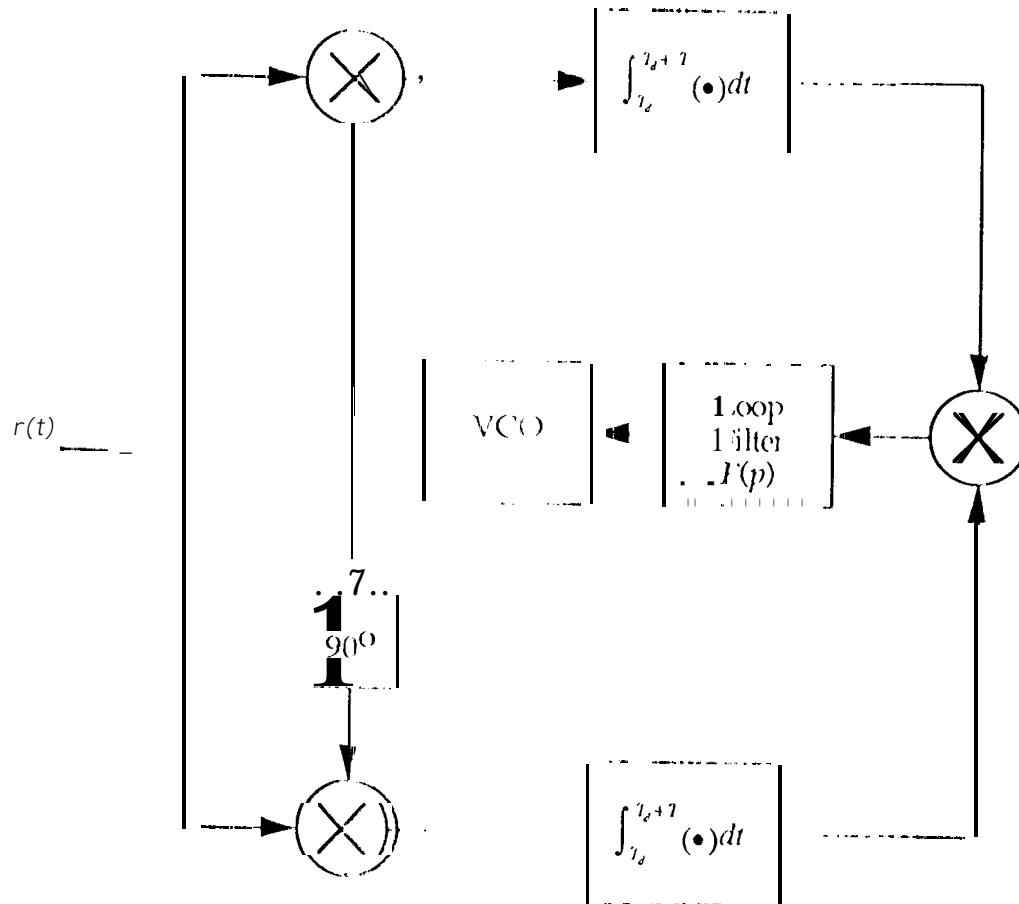


Fig. 4 Conventional (wideband) I-Q Loop

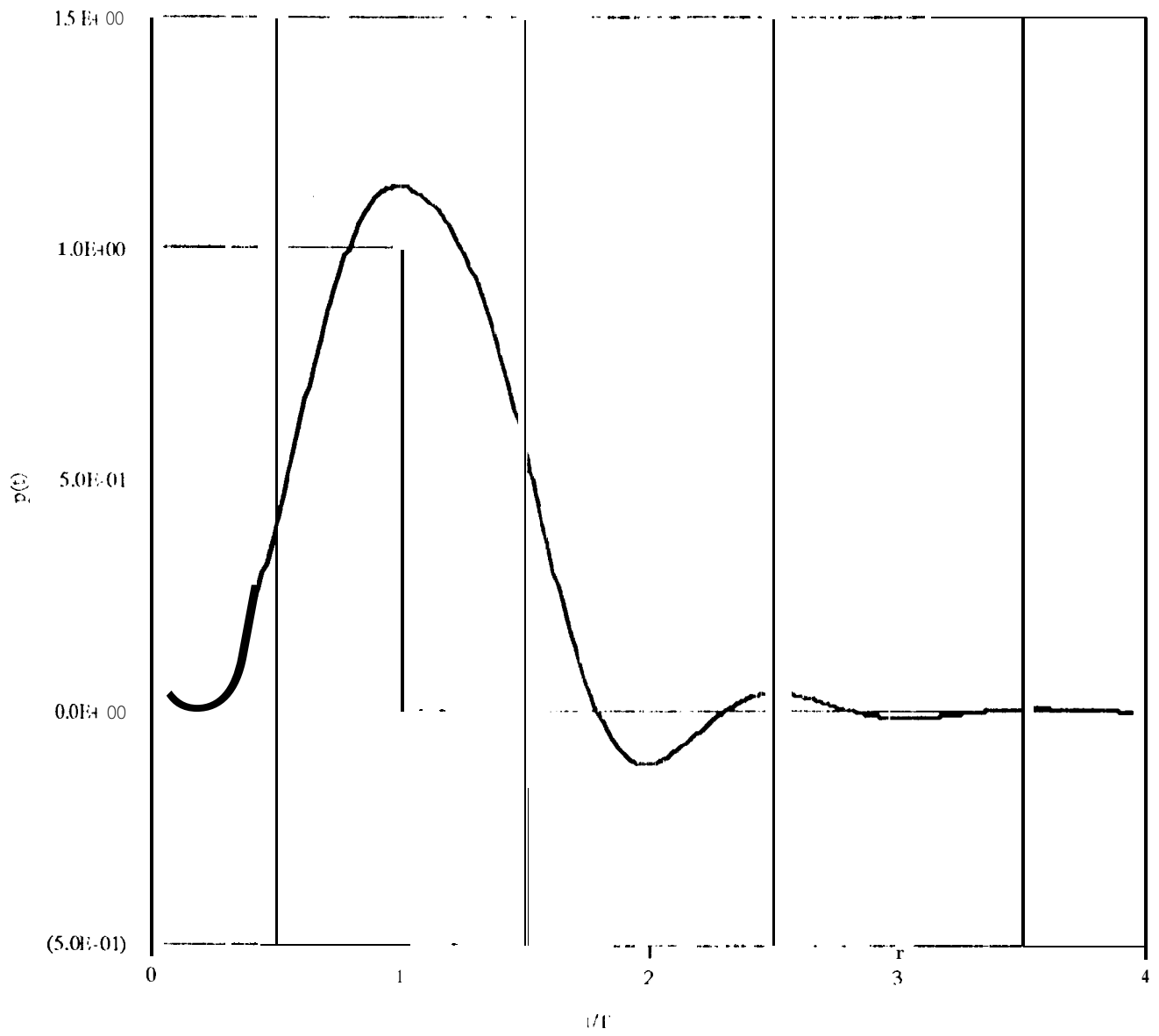


Fig. 5 Pulse response of a 5 pole Butterworth filter to a T -sec rectangular pulse

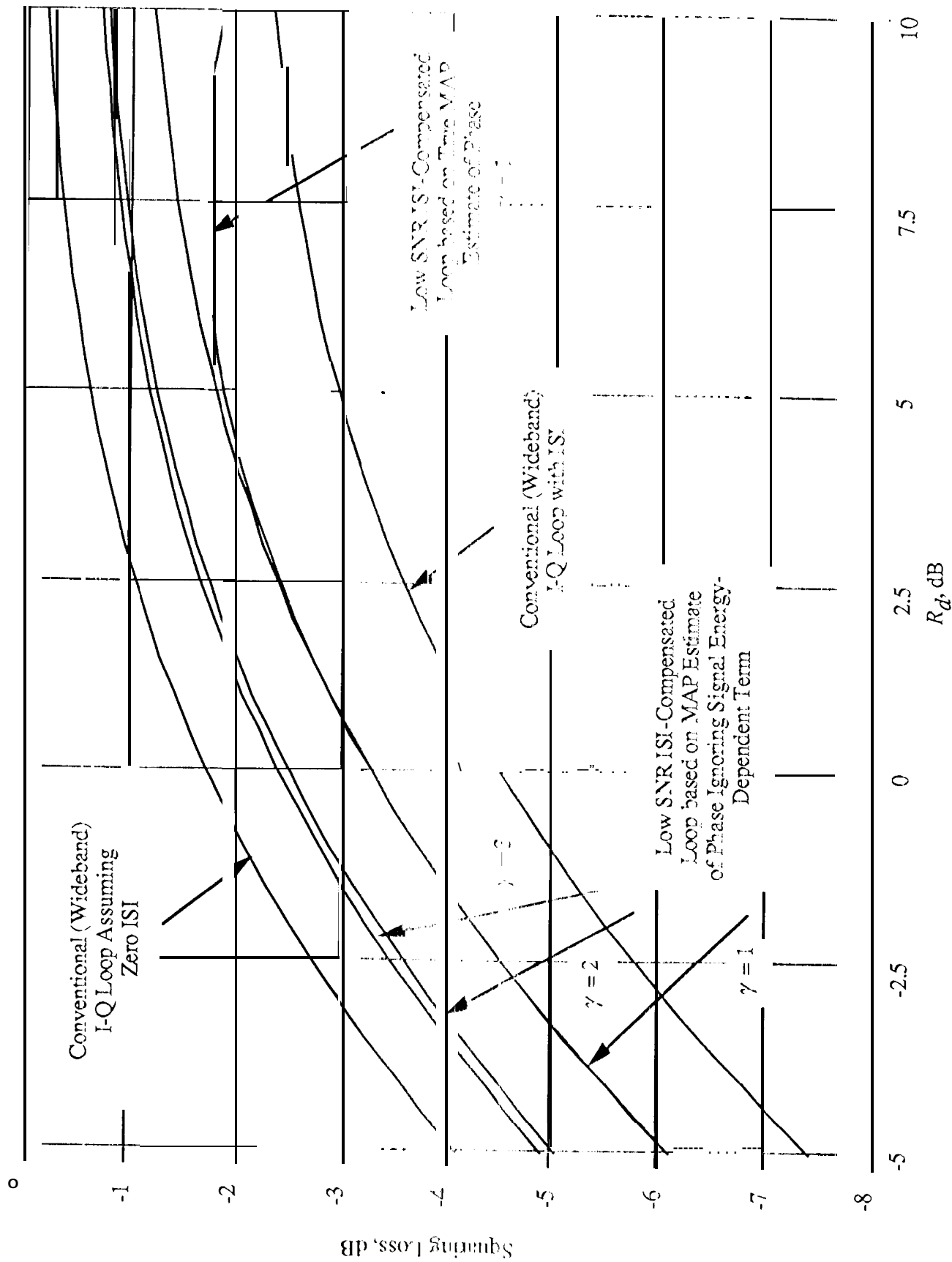


Fig. 6a. Squaring Loss Performance of ISI-Compensated I-Q Loops; SI Created by 5-Pole Butterworth Filter ($T_d = \infty.25$)

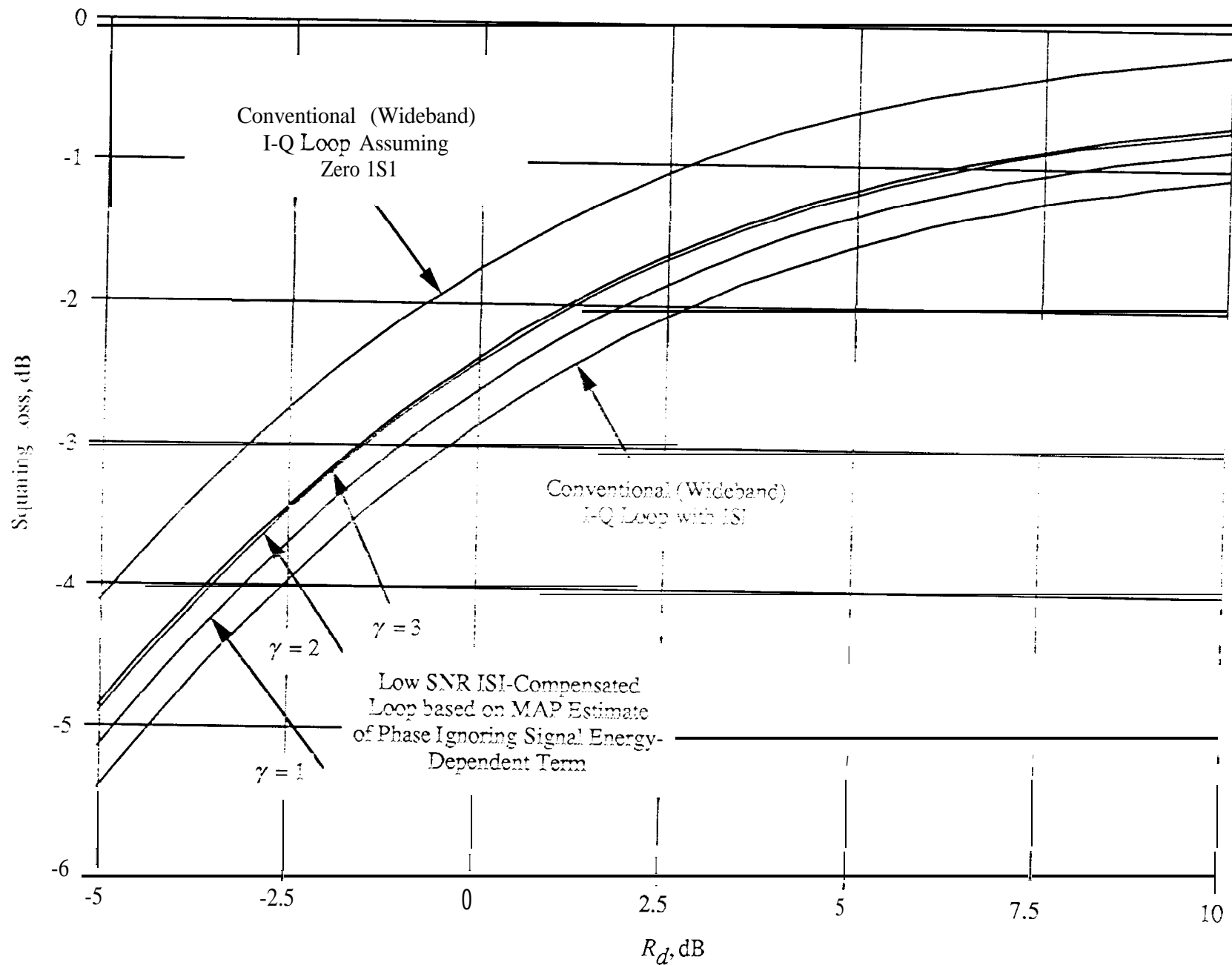


Fig. 6b. Squaring Loss Performance of ISI-Compensated I-Q Loops: ISI Created by 5-Pole Butterworth Filter ($T_d = 0.50$)

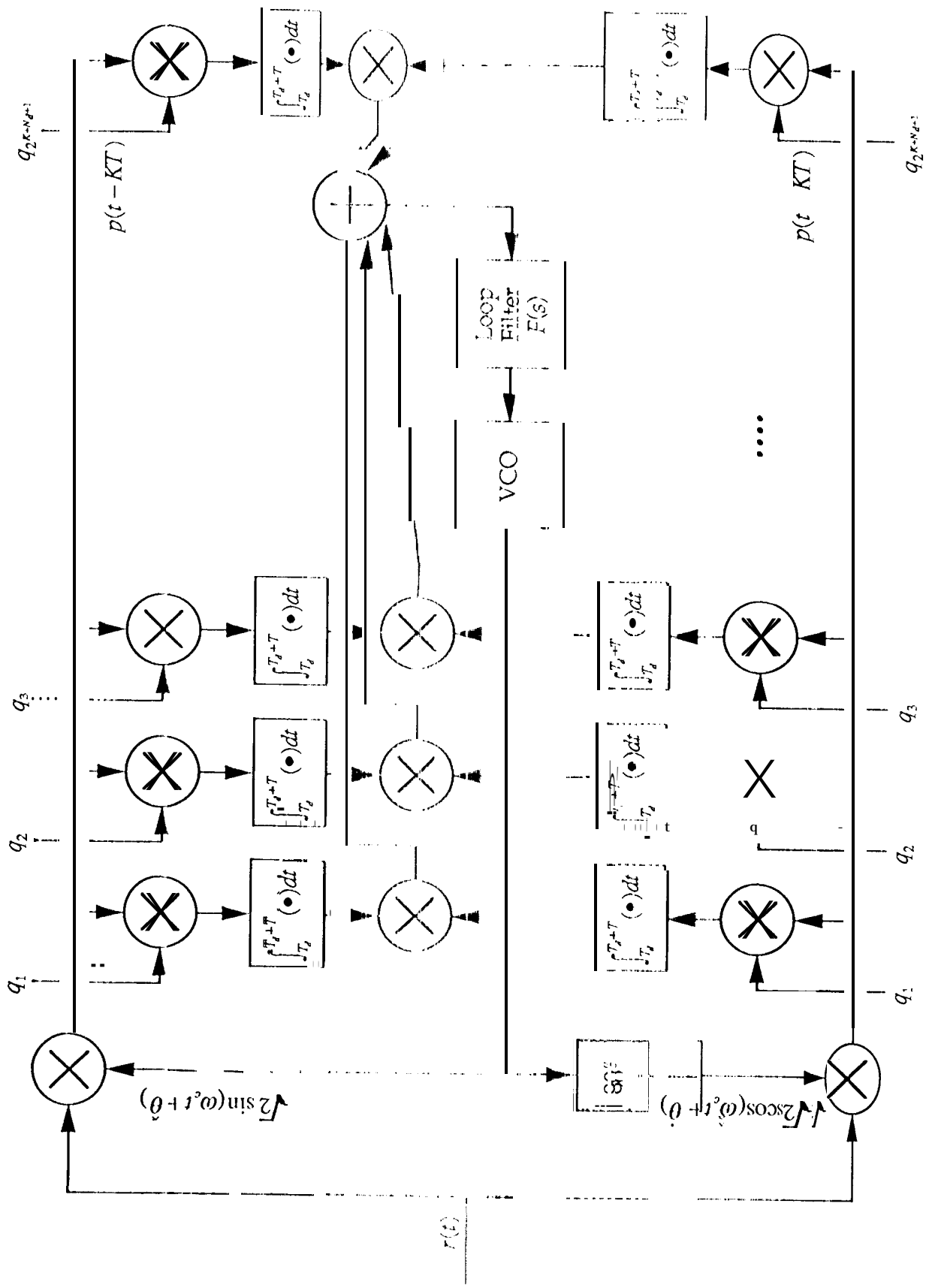


Fig. 7a Block Diagram of Optimum (Low SNR) ISI-Compensated I-Q Loop

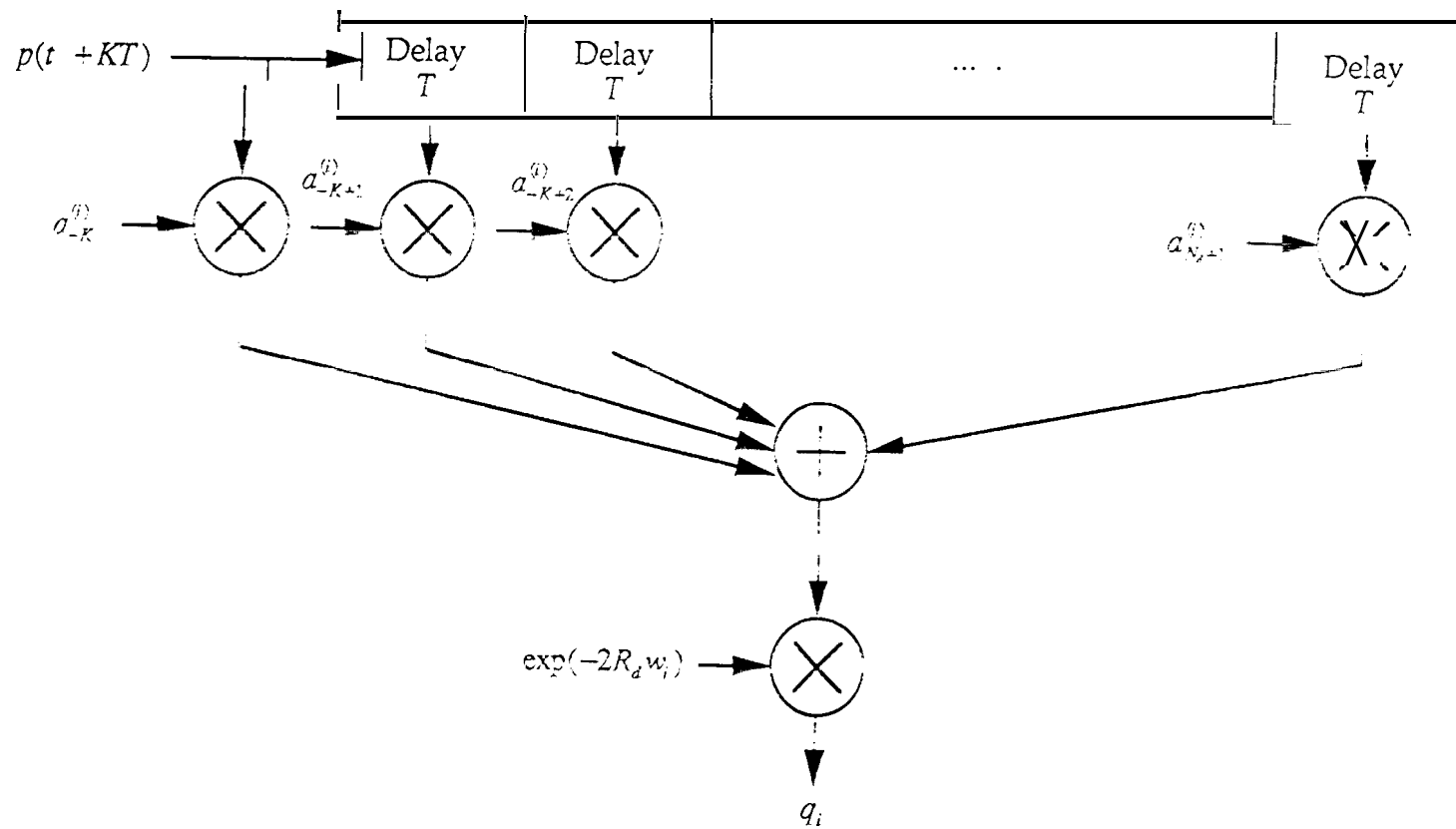


Fig. 7b Block Diagram of Circuit for Generating $q_i; i = 1, 2, \dots, 2^{K+N_d+1}$